Direct measurement of the $\bar{K}N \to \pi\Sigma$ scattering amplitude below the $\bar{K}N$ threshold employing the $d(K^-, N)"\pi\Sigma"$ reaction

Kentaro Inoue

July 25, 2025

Contents

Chapter 1

Introduction

1.1 Discovery of the $\Lambda(1405)$

The $\Lambda(1405)$ is a hyperon with strangeness $S = -1$, isospin $I = 0$ and spin and spin parity $J^P = (\frac{1}{2})^-$. In the Particle Data Group (PDG) [1], the mass and the width of the $\Lambda(1405)$ are assigned to $1405.1^{+1.3}_{-1.0}$MeV and 50.5 ± 2.0MeV respectively, based on several papers [2–4].

The existence of the $\Lambda(1405)$ was predicted for the first time by R. H. Dalitz and S. F. Taun in 1959 as a quasi-bound state of $\bar{K}N$ [5]. The candidate was reported in the $K^-p \to \pi\pi\pi\Sigma$ reaction at the Lawrence Radiation Laboratory in 1961 [6]. The excess was reported in the neutral $\pi\Sigma$ spectrum, $K^-p \to \pi^\pm\pi^\mp(\pi\Sigma)^0$, in the $\Lambda(1405)$ region compared to the doubly charged spectrum, $K^-p \to \pi^+\pi^+(\pi^-\Sigma^-)$ or $K^-p \to \pi^-\pi^-(\pi^+\Sigma^+)$, in this paper. However, there was not enough statistical data to discuss lineshape. In order to solve these problems, R. J. Hemingway reported high-statistics $\pi^+\Sigma^-$ and $\pi^-\Sigma^+$ spectra using the $K^-p \to \pi^-\Sigma^+(1660) \to \pi^-\pi^+(\pi^\mp\Sigma^\pm)$ with 4.2 GeV/c K^- beam [7]. In these spectra, the momentum transfer was restricted to, $t(K^-, \pi^-)$ <1.0 GeV/c, in order to increase the purity of $\Sigma^+(1660)$. As a result, the $\Sigma^+ \to \pi^0 p$ decay event of the $K^-p \to \pi^-\Sigma^+(1660) \to \pi^-\pi^+(\pi^-\Sigma^+)$ reaction gave a $\pi^-\Sigma^+$ spectrum with almost no background. R. H. Dalitz and A. Deloff obtained the mass and width of the $\Lambda(1405)$ as 1406.4 ± 4.0 MeV and 50 ± 2 MeV [2] by adapting the M-matrix method to this spectrum, and these parameters were adopted for the PDG. On the other hand, the $\pi^+\Sigma^-$ spectrum of the $K^-p \to \pi^-\Sigma^+(1660) \to \pi^-\pi^+(\pi^+\Sigma^-)$ reaction had a background due to the ambiguity of the origin of the π^-. Thus, the mass spectrum of $\Lambda(1405)$ was investigated using the K^-p reaction with pion emission.

1.2 $\bar{K}N$ interaction

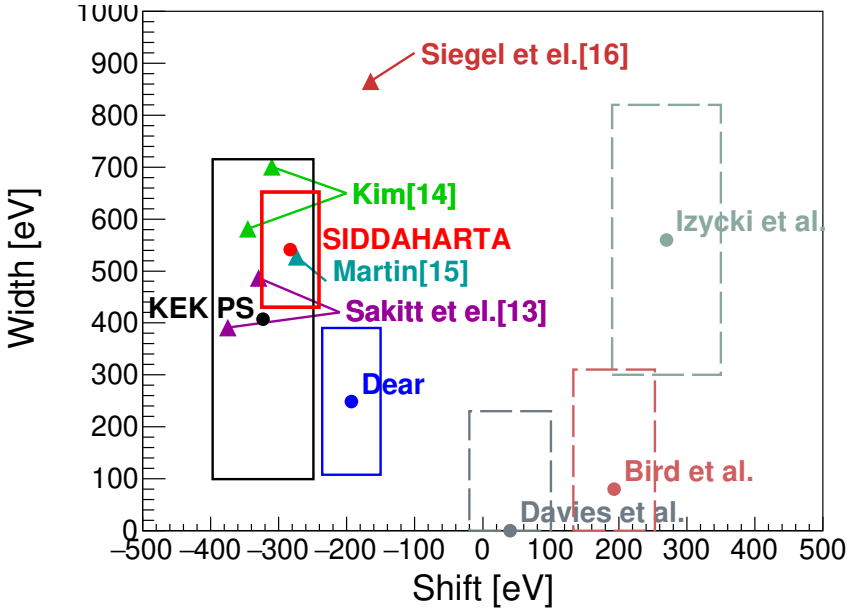

Figure 1.1: This figure is shown about the kaonic hydrogen. Triangle markers indicate theoretical calculations where $\bar{K}N$ scattering data were extrapolated to the $\bar{K}N$ threshold. Circle markers represent experimental values, and error ranges in the energy shift and width are indicated by squares. Dashed lines correspond to experiments using hydrogen gas targets conducted prior to 1990, while solid lines represent experiments conducted afterward.

Considering the $\Lambda(1405)$ as a $\bar{K}N$ bound state, the $\bar{K}N$ interaction is expected to be attractive. From the 1960's to the 1980's, various $K^-p \to$ meson-baryon, e.g., K^-p, K^0n, $\pi\Lambda$, $\pi\Sigma$, and so on, scattering data were measured on a hydrogen target using bubble chambers to study the $\bar{K}N$ interaction [8–12]. This method of course did not allow access below the $\bar{K}N$ mass threshold and measurements in the low momentum region were difficult and data were insufficient. Nevertheless, the value of the $\bar{K}N$ interaction at the $\bar{K}N$ mass threshold was obtained by extrapolating it from the high momentum region, where abundant data exist, using several models [13–16]. These values are shown in Figure 1.1 as the characteristic X-ray values for kaonic hydrogen, discussed below. Due to the lack of data in the low

momentum region, these values varied. However, they were all attractive and consistent with the $\Lambda(1405)$ being a $\bar{K}N$ bound state.

An attempt to measure $\bar{K}N$ interactions at the $\bar{K}N$ mass threshold using kaonic hydrogen has been proposed. In this method, a K^- meson beam is stopped in a hydrogen target, and the characteristic X-rays emitted when the kaon binds to a proton are utilized. In the case of nucleon-meson, the characteristic X-ray is affected not only by electromagnetic interactions but also by the strong interactions i.e. $\bar{K}N$ interaction, leading to a shift in energy and a gain in width compared to the case where only electromagnetic interactions are present. According to Deser-Trueman formula [36, 37], these shift and width are model-independent and given by $\Delta E_1^s - \frac{i}{2}\Gamma_1 = -2\alpha^3\mu_c^2 a_{K^-p}$. Where α is the fine structure constant, μ_c is the mass of the K^--p system, and a_{K^-p} is the scattering length of the $\bar{K}N$ interaction. Several attempts were made in the 1980s using liquid hydrogen targets [17–19]., but the results showed a positive energy shift, indicating that the $\bar{K}N$ interaction is repulsive, contradicting $\bar{K}N$ scattering experiments. To improve the poor signal-to-noise ratio of these experiments, experiments were conducted at KEK PS using gaseous hydrogen targets, and a negative energy shift was reported, thus confirming that the $\bar{K}N$ interaction is attractive [20].

Once the $\bar{K}N$ scattering experiments and characteristic X-ray measurements were found to be qualitatively consistent, this led to further investigations into the $\bar{K}N$ interaction. The scattering length from characteristic X-ray measurements was determined more precisely by DEAR [35] and the SIDDHARTA Collaboration [21]. The values of these experiments are also shown in Figure 1.1. The SIDDHARTA data serve as a crucial constraint on the $\bar{K}N$ mass threshold, playing a key role in constraining the $\bar{K}N$ scattering amplitudes discussed later.

1.3 Two pole strcture of the $\Lambda(1405)$

A theoretical extrapolation of the $\bar{K}N$ scattering amplitude to the low-momentum regime was made in an effort to better understand the low-energy behavior. However, applying a low-momentum perturbation expansion to the strangeness sector proved to be challenging due to the presence of $\Lambda(1405)$.

This model suggested that $\Lambda(1405)$ receives contributions from two poles [27]: one being a bound state located in the high-mass region of the $\bar{K}N$ system at $1426 + 16i$ MeV, and the other being a resonant state of the $\pi\Sigma$

system located in the low-mass region at $1390 + 66i$ MeV. Due to contributions from both poles, the spectral shape and intensity of $\Lambda(1405)$ are expected to depend on the reaction mechanism and the $\pi\Sigma$ decay modes. Therefore, it is important to collect data on various $\pi\Sigma$ modes through the use of different reaction mechanisms.

1.4 Recent experimental status of the $\Lambda(1405)$

Experiments using two reaction mechanisms were conducted in this context. One is photoproduction, $\gamma p \to K^+\Lambda(1405)$, and the other is proton-proton collisions, $pp \to nK^+\Lambda(1405)$.

The photoproduction experiment was first performed at LEPS using a 1.5-2.4 GeV γ-ray beam, where the $\pi^-\Sigma^+$ and $\pi^+\Sigma^-$ spectra were reported [23]. The difference between these two spectra was attributed to the interference between the $I = 0$ and $I = 1$ components, and this interference term was observed. Subsequently, the CLAS Collaboration reported the spectra of all three $\pi\Sigma$ modes, i.e., $\pi^-\Sigma^+$, $\pi^+\Sigma^-$ and $\pi^0\Sigma^0$, using 1.61-1.91 GeV γ-ray beams, and all three spectral shapes were different [24]. They also experimentally confirmed that $\Lambda(1405)$ has isospin $I = 0$ and spin-parity $I^P = (\frac{1}{2}^-)$ [25]. Those three spectra were reproduced by theoretical calculations of the photoproduction process using the chiral unitary model [26]. However, in these calculations, some phenomenological parameters were adjusted by fitting the spectra, indicating that the photoproduction process is complex and that it is not possible to conclude how the $\Lambda(1405)$ poles affect the spectra.

Results from proton-proton scattering were reported by the HADES collaboration using proton beam with 3.5 GeV, which presented spectra of $\pi^-\Sigma^+$ and $\pi^+\Sigma^-$ [28]. Differences were observed in these spectra, indicating that $I = 0$ and $I = 1$ interference was also present in proton-proton scattering. The peaks of these two spectra are clearly located below 1400 MeV, indicating that the peak position of $\Lambda(1405)$ strongly depends on the production mechanism. However, as in the case of photoproduction, the production mechanism of $\Lambda(1405)$ in proton-proton scattering is complex, and it is not possible to conclude how its poles affect the spectrum.

1.5 Recent theoritical status of the $\Lambda(1405)$

Although the various experiments described above do not provide conclusive information on the poles of $\Lambda(1405)$, they play an important role in

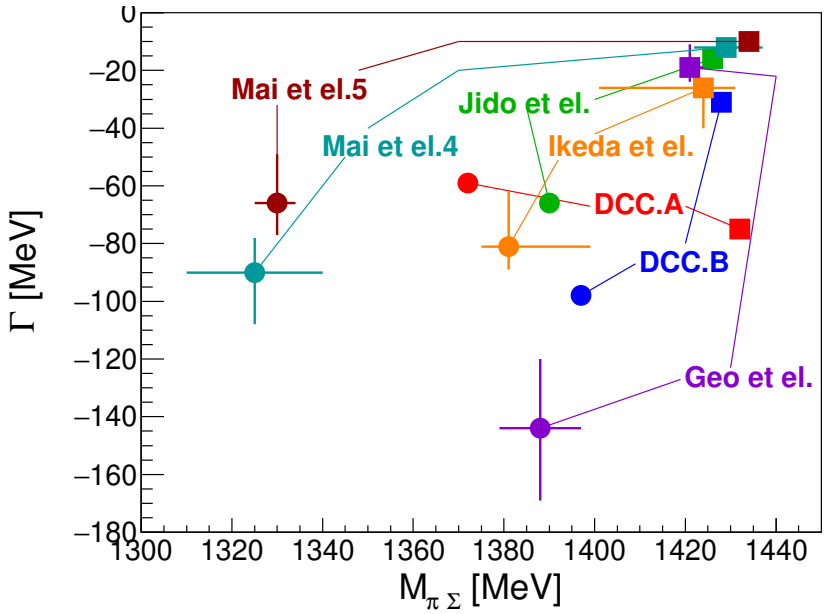

Figure 1.2: This figure shows the pole structure with $I = 0$ $\bar{K}N$ scattering amplitudes below the $\bar{K}N$ threshold by various theoritical analysis.

theoretical studies. Building on these results, theoretical studies based on the chiral unitary model have aimed to obtain more detailed $\bar{K}N$ scattering amplitudes while imposing chiral symmetry and unitarity conditions.

Y. Ikeda et al. [29] and Z.-H. Geo et al. [30] theoretically calculated the $\bar{K}N$ scattering amplitudes by incorporating not only the results of $\bar{K}N$ scattering experiments but also the SIDDARTA experimental results as constraints, including not only the leading order but also the next-to-leading (NLO) order in their analysis. M. Mai et al. derived several solutions through a similar analysis and tested them against the results of the CLAS experiment [31]. However, since the CLAS experimental data require reaction-specific calculations for fitting, they could not be directly incorporated into the fitting procedure. Instead, they were used as a filter to evaluate the resulting solutions, leaving two viable candidates.

Since chiral unitary calculations are based on perturbative expansions at low momentum, low-momentum $\bar{K}N$ scattering data have been primarily used. However, due to experimental difficulties, the available low-momentum data are insufficient, whereas medium- to high-momentum scattering data are more abundant. Partial wave analysis is known as a method applicable to this energy region and has been extensively studied, as described in Section 1.2. It continues to evolve with the incorporation of new data [32, 33]. However, even with this approach, drawing conclusions at low momentum has been difficult due to the presence of $\Lambda(1405)$. To overcome this challenge, the $\bar{K}N$ scattering amplitudes analyzed using the DCC model, a dynamic extension of partial wave analysis, were reported [34]. The analysis produced two solutions for the scattering amplitudes, primarily due to the lack of data in the low-momentum region. Although both scattering amplitudes exhibit two poles in the S-wave scattering below the $\bar{K}N$ mass threshold, similar to the chiral unitary model, the parameters of these poles were very different. The pole positions of $\Lambda(1405)$ based on the theoretical analysis presented in this chapter are summarized in Figure 1.2.

1.6 $d(K^-, n)$ reaction

Given the aforementioned circumstances, it is strongly desired to measure direct $\bar{K}N$ scattering data in the mass region of $\Lambda(1405)$. However, if the scattered $\bar{K}$ meson and nucleon are detected as free particles after $\bar{K}N$ scattering, scattering amplitudes below the $\bar{K}N$ mass threshold cannot be obtained. As stated in Section 1.2, while the K^-p reaction provides scattering data above the $\bar{K}N$ mass threshold, it cannot provide scattering amplitudes

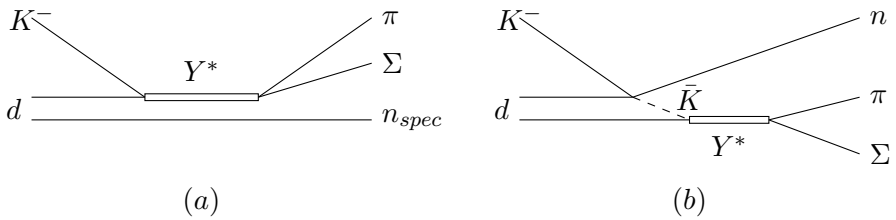

(a) (b)

Figure 1.3: This figure is a diagram of the $K^-d \to n\Sigma\pi$ reaction. The left figure (a) represents a one-nucleon reaction, and the right figure (b) represents a two-step reaction.

below the threshold due to energy conservation. Thus, the $K^-d \to nY^*$ reaction with a deuterium target can be used, in which Y^* can be produced below the $\bar{K}N$ mass threshold by transferring the energy of the K^- beam to the neutron.

Experiments using this reaction were conducted at CERN by irradiating a liquid deuterium target with a K^- beam having a momentum of 686-844 MeV/c [38]. Although only the spectrum of the $\pi^+\Sigma^-$ mode was reported in this experiment, the spectrum showed a peak around 1420 MeV, which is higher than the conventional peak position of $\Lambda(1405)$. Since this reaction is $\bar{K}$-induced, it is considered to strongly reflect the $\bar{K}N$ pole, which is consistent with the chiral unitary model. In fact, D. Jido et al. used the chiral unitary model to calculate the $K^-d \to n\Sigma\pi$ reaction and successfully reproduced the experimental spectrum [39]. However, their calculation also required the P-wave $\Sigma(1385)$ contribution at $I = 1$. The $\pi\Sigma$ spectrum is reported only for $\pi^+\Sigma^-$ in this experiment, but a $\pi^-\Lambda$ spectrum from the $K^-d \to p\Lambda\pi^-$ reaction was also reported. Since this spectrum corresponds to $I = 1$, it does not include a $\Lambda(1405)$ contribution but does contain a $\Sigma(1385)$ contribution. J. Yamagata et al. reproduced the $\pi^-\Lambda$ spectrum of this experiment using the same reaction calculation framework [40]. Thus, this experiment provides strong support for the validity of the chiral unitary model.

Two types of reactions are possible for this process: a one-nucleon reaction (a) and a two-step reaction (b), as shown in Figure 1.3. These two reactions are kinematically distinguishable, but not in this experiment, where all Y$*$ production angles were measured. Nevertheless, neutrons originating from Fermi motion, which do not contribute directly to the reaction, are emitted in all directions. Therefore, the one-nucleon reaction is considered to play a more significant contribution in this experiment.

Summarized, only the $\pi^-\Sigma^+$ spectrum was reported in this experiment, and the reaction mechanism remained unknown. The J-PARC E31 experiment was planned to address this issue.

1.7 The J-PARC E31 experiment

The J-PARC E31 experiment employs a two-step reaction, as shown in Figure 1.3-(b). In this reaction, the irradiated K^- beam knocks out a nucleon in deuterium, which are then scattered forward. In addition, a Cylindrical Detector System (CDS) is installed around the liquid deuterium target to identify the $\pi\Sigma$ decay mode, and the particles originating from the decay of the produced Y^* will be measured. In this experiment, a 1 GeV/c K^- beam is used, which frequently undergoes $K^-N \to \bar{K}N$ elastic scattering. When the missing mass of Y^* produced in this reaction is near the $\bar{K}N$ threshold, the momentum of the scattered $\bar{K}$ is around 250 MeV/c, making it easier to induce a secondary reaction with the residual nucleon.

In this experiment, all $\pi\Sigma$ modes are measured, i.e., the $\pi^-\Sigma^+$, $\pi^0\Sigma^0$, and $\pi^+\Sigma^-$ spectra. However, this paper focuses on discussing the $\pi^-\Sigma^+$ and $\pi^+\Sigma^-$ spectra. These spectra include contributions from $I = 0$ and $I = 1$ states, and their interference terms. However, using only these two spectra, it is impossible to fully disentangle the individual contributions. Therefore, we also discuss the $K^-d \to p\pi^-\Sigma^0$ spectrum, in which the proton is detected in the forward direction. This spectrum is purely associated with $I = 1$, and by incorporating this information, the $I = 0$, $I = 1$, and interference component can be fully disentangled.

One such calculation was performed by Miyagawa et al [42]. They used the scattering amplitudes from the latest partial-wave analysis for the first-step $\bar{K}N \to \bar{K}N$ scattering and those from some chiral unitary approaches for the second-step $\bar{K}N \to \pi\Sigma$ scattering. Thus, their calculation adopts a *hybrid* method that combines two different approaches. This is because the chiral unitary approach is specialized for low-energy interactions and is not applicable to the first-step $\bar{K}N \to \bar{K}N$ scattering. The spectrum of this experiment, considering the same two-step scattering process, has also been calculated using the DCC model. As mentioned in Section 1.5, this model extends the partial-wave analysis, which had been difficult to apply to the $\Lambda(1405)$ region, thereby making it applicable to that region.

The setup for this experiment, briefly introduced at the beginning of this chapter, is detailed in Chapter **??**. The calibration and analysis methods for the detectors are described in Chapter **??**. The selection of $\pi\Sigma$

modes from the measured data and their conversion to cross sections are discribed in Chapter **??**. The physical interpretation of the obtained spectra is discussed in Chapter **??**. There, we discuss how well $\bar{K}N$ scattering is understood by comparing it with the theoretical calculations presented in this chapter, especially in the region of $\Lambda(1405)$. In doing so, we examine the contribution of each component by decomposing it into $I = 0$, $I = 1$, and their interference terms. Finally, using the $I = 0$ spectrum obtained from this experiment, we determine its scattering length and effective range, from which we derive the pole parameters of $\Lambda(1405)$, namely its mass and width.

Chapter 2

Experimental setup

Chapter 3

Analysis

Chapter 4

Discussion

4.1 Decomposition of the $K^- d \to n\pi^+\pi^- n$ events

4.1.1 Backward $\pi^\mp\Sigma^\pm$ event selection

4.1.2 Template fitting

4.2 Conversion to the cross section

4.3 Spectra

4.3.1 Qualitative properties of obtained spectra

4.3.2 Comparison with theoritical calculations

4.3.3 $\bar{K}N$ Pole parameters assuming the 2-step reaction

4.3.4 Comparison with DCC model

Chapter 5

Conclusion

Appendix A

$\pi^0\Sigma^0$ spectrum analysis

Appendix B

Detector resolution

B.1 CDC resolution

B.2 Detector resolution on the $d(K^-, N)$

Appendix C

$d(K^-, n)K^0n$ analysis

Bibliography

[1] R.L. Workman et al. (Particle Data Group), Prog. Theor. Exp. Phys. 2022, 083C01 (2022)
"Review of Particle Physics"

[2] R. H. Dalitz and A. Deloff, J. Phys. G17, 281 (1991).
"The Shape and Parameters of the $\Lambda(1405)$ Resonance"

[3] M. Hassanvand et el., Phys. Rev. C **87**, 055202 (2013)
"Theoretical analysis of $\Lambda(1405) \to (\pi\Sigma)^0$ mass spectra produced in $p + p \to p + \Lambda(1405) + p$ reactions"

[4] J. Esmaili, Y. Akaishi, and T. Yamazaki, Phys. Lett. B **686**, 23 (2010)
"Experimental confirmation of the $\Lambda(1405)$ ansatz from resonant formation of a $K^- p$ quasi-bound state in K^- absorption by ^{3}He and ^{4}He"

[5] R. H. Dalitz and S. F. Tuan, Phys. Rev. Lett. 2 (1959).
"Possible Resonant State in Pion-Hyperon Scattering"

[6] M. H. Alston, L. W. Alvarez, P. Eberhard and M. L. Good,
Phys. Rev. Lett. 6, 698 (1961).
"Study of Resonances of the Σ-π System"

[7] R. J. Hemingway, Nucl Phys B **253**, 742 (1985).
"Production of $\Lambda(1405)$ in $K^- p$ Reactions at 4.2GeV/c"

[8] B. Conforto et el., Nucl. Phys. B **34**, 41 (1971).
"New experimental results on the Reactions $K^- p \to \bar{K} N$ and $K^- p \to \Sigma\pi$ a partial-wave analysis between 430 and 800MeV/c"

[9] A. J. Van Horn, Nucl. Phys. B **87**, 145 (1975).
"Energy dependent partial-wave analysis of $K^- p \to \Lambda\pi^0$ between1540 and 2215MeV"

[10] R. J. Hemingway et el., Nucl. Phys. B **91**, 12 (1975).
"New data on $K^-p \to K^-p$ and K^0n and a partial-wave analysis between 1840 and 2234MeV center of mass energy"

[11] P. Baillon and P. J. Litchfield, Nucl. Phys. B **94**, 39 (1975).
"Energy-independent partial-wave analysis of $\bar{K}N \to \Lambda\pi$ between 1540 and 2150 MeV"

[12] G. P. Gopal et al., Nucl. Phys. B **119**, 362 (1977).
"Partial-wave analyses of KN two-body reactions between 1480 and 2170 MeV"

[13] M. Sakitt et el., Phys. Rev. **139**, B179
"Low-Energy K^- Meson Interactions in Hydrogen"

[14] J. K. Kim, Phys. Rev. Lett. **19**, 1074 (1967).
"Multichannel Phase-Shift Analysis of $\bar{K}N$ Interaction in the Region 0 to 550 MeV/c"

[15] A. D. Martin, Nucl. Phys. B **179**, 33 (1981).
"Kaon-Nucleon Parameters"

[16] P. B. Siegel and W. Weise, Phys. Rev. C **38**, 2221 (1988).
"Low-energy K^--nucleon potentials and the nature of the $\Lambda(1405)$"

[17] J. D. Davies et al., Phys. Lett. B **83**, 55 (1979).
"Observation of kaonic hydrogen atom X-rays"

[18] M. Izycki et al., Z. Phys. A 297, 11 (1980).
"Results of the search for K-series X-rays from kaonic hydrogen"

[19] P. M. Bird et al., Nucl. Phys. A **404**, 482 (1983).
"Kaonic Hydrogen atom X-rays"

[20] M. Iwasaki et el., Phys. Rev. Lett. **78**, 3067 (1997).
"Observation of Kaonic Hydrogen K_α X Rays"

[21] M. Bazzi et el., Phys. Lett. B **704**, 113 (2011).
"A New Measuerment of Kaonic Hydrogen X-Rays"

[22] J.C.Nacher et el., Phys. Lett. B **455**, 55 (1999).
"Photoproduction of the $\Lambda(1405)$ on the proton and nuclei"

[23] M. Niiyama et el., Phys. Rev. C **78**, 035202 (2008).
"Photoproduction of $\Lambda(1405)$ and $\Sigma(1385)$ on the proton at $E_\gamma = 1.5$-2.4GeV/c"

[24] K. Moria for the CLAS Collaboration,
Phys. Rev. C **87**, 035206 (2013).
"Measurement of the $\pi\Sigma$ photoproduction line shapes near the $\Lambda(1405)$"

[25] K. Moria for the CLAS Collaboration,
Phys. Rev. Lett. **112**, 082004 (2014).
"Spin and parity measurement of the $\Lambda(1405)$ baryon"

[26] S. X. Nakamura, and D. Jido, Prog. Theor. Exp. Phys., 023D01 (2014)
"Lambda (1405) photoproduction based on the chiral unitary model"

[27] D. Jido et el., Nucl. Phys. A **725**, 181 (2003).
"Chiral Dynamics of the Two $\Lambda(1405)$ States"

[28] G. Agakishiev for the HADES Collaboration,
Phys. Rev C **87**, 025201 (2013).
"Baryonic Resonances to the $\bar{K}N$ threshold: The case of $\Lambda(1405)$ in pp collisions"

[29] Y. Ikeda, T. Hyodo, and W. Weise, Nucl. Phys. A **881**, 98 (2012)
"Chiral SU(3) theory of antikaon–nucleon interactions with improved threshold constraints"

[30] Z.-H. Guo and J. Oller, Phys. Rev. C **87**, 3, 035202 (2013)
"Meson-baryon reactions with strangeness -1 within a chiral framework"

[31] M. Mai and U.-G. Meißner, Eur. Phys. J. A **51**, 3, 30 (2015),
"Constraints on the chiral unitary amplitude from $\pi\Sigma K^+$ photoproduction data"

[32] H. Zhang et el., Phys. Rev. C **88**, 035204 (2013).
"Partial-wave analysis of $\bar{K}N$ scattering reactions"

[33] H. Zhang et el., Phys. Rev. C **88**, 035205 (2013).
"Multichannel parametrization of $\bar{K}N$ scattering amplitudes and extraction of resonance parameters"

[34] H. Kamano et el., Phys. Rev. C **90**, 065202 (2014).
"Dynamical Coupled-Channels Model of K^-p Reactions:

Determination of partial wave aamplitudes"
Phys. Rev. C**92**, 025205 (2015).
"Dynamical Coupled-Channels Model of K^-p Reactions. II
Extraction of Λ^* and Σ^* Hyperon Resonances"
Phys. ReV. C**95**, 044903(E) (2015).

[35] G. Beer et el., Phys. Rev. Lett. **94**, 212302 (2005).
"Measurement of the Kaonic Hydrogen X-Ray Spectrum"

[36] S. Deser et el., Phys. Rev. **96**, 774 (1954).
"Energy Level Displacements in Pi-Mesonic Atoms"

[37] T.L. Trueman, Nucl. Phys. **26**, 57 (1961).
"Energy level shifts in atomic states of strongly-interacting particles"

[38] O. Braun et el., Nucl. Phys. B **129**, 1 (1977).
"New Information About the Kaon-Nucleon-Hyperon Coupling Constants $g(KN\Sigma(1197)), g(KN\Sigma(1385))$ and $g(KN\Lambda(1405))$"

[39] D. Jido, E. Oset and T. Sekihara, Eur. Phys. J. A **42**, 257 (2009).
"Kaonic Production of $\Lambda(1405)$ off deuteron target in chiral dynamics"

[40] J. Yamagata-Sekihara, T. Seki hara, and D. Jido, Prog. Theor. Exp. Phys.**2013**, 043D02 (2013).
"Production of hyperon resonances induced by kaons on a deuteron target"

[41] H. Noumi et el., Proposals for the 15th PAC meeting
"Spectroscopic study of hyperon resonances below $\bar{K}N$ threshold via the (K^-, n) reaction on Deuteron"

[42] K. Miyagawa, J. Haidenbauer, and H. Kamada Phys. Rev. C **97**, 055209 (2018)
"Faddev approach to the reaction $K - d \to \pi\Sigma n$ at $p_K = 1.0GeV/c$"

[43] E. Oset, A. Ramos, and C. Bennhold, Phys. Lett. B **527**, 99 (2002); **530**, 260(E) (2002).
"Low lying $S = -1$ excited baryons and chiral symmetry"

[44] A. Cieplý and J. Smejkal, Nucl. Phys. A **881**, 115 (2012).
"Chirally motivated $\bar{K}N$ amplitudes for in-medium applications"

[45] S. Ohnishi et el, Phys. Rev. C **93**, 025207 (2016).
"Strcture of the $\Lambda(1405)$ and the $K^- d \to \pi\Sigma n$ reaction"

[46] H. Kamano et el., Phys. ReV. C**94**, 065205 (2016).
"Toward Establishing Low-Lying Λ and Σ Hyperon Resonances with the $\bar{K} + d \to \pi + Y + N$ Reaction"

[47] H. Noumi for the E31 Collaboration, Phys. ReV. B**837**, 137637 (2023).
"Pole Position of $\Lambda(1405)$ measured in $d(K^-, n)\pi\Sigma$ reaction"

[48] S. Kawasaki's Doctor thesis will be submitted.

[49] K. Agari et el, Prog. Theor. Exp. Phys., 02B009 (2012)

[50] K. Agari et el, Prog. Theor. Exp. Phys., 02B011 (2012)

[51] TRANSPORT http://linac96.web.cern.ch/Linac96/Proceedings/Thursday/THP72/Paper.pd

[52] T. K. Ohska et al., Nuclear Science, IEEE Transactions on 33, 98 (1986).

[53] M. Shiozawa and et el., A new TKO system manager board for a dead-time-free data acquisition system, in 1994 IEEE Nuclear Science Symposium-NSS'94, pages 632–635, (1994)

[54] M. Iio et al., Nucl. Instrum. Methods Phys. Res., Sect. **A** 687, 1 (2012).

[55] S. Agostinelli et al., Nucl. Instrum. Methods Phys. Res., Sect. **A** 506, 250 (2003)
J. Allison et el., IEEE Transactions on Phys. Sci. 53, 207 (2006)
J.Allison et al., Nucl. Instrum. Methods Phys. Res., Sect. **A** 835, 186 (2016)

[56] K. Fuji, `https://www-jlc.kek.jp/subg/offl/lib/docs/helix_manip/node3.html` (1968).

[57] Opera Electromagnetic FEA Solution Software

[58] V. Flaminio et al., CERN-HARA-87-01, 121 (1983).

[59] M.Jones et el, Nucl. Phys. B **90**, 349 (1975)

[60] R. Barlow and C. Beeston, Comp. Phys. Comm. **77**, 219 (1993).
"Fitting using finite Monte Carlo samples"

[61] A. Nappi, Comp. Phys. Comm. **180**, 269 (2009).

[62] C.J.S. Damerell et. el., Ncul. Phys. B**129**, 397 (1977). "
K^-n elastic scattering between 610 and 840 MeV/c"

[63] M. jones, R. Levi, Setti, D. Merrill and R. D. Tripp, Phys. Rev. B**90**, 349 (1975). K^-p charge exchange and hyperon production cross section from 860 to 1000 MeV/c

[64] M. Bernheim and et. el., Nucl. Phys. A**365**, 349, (1981). Momentum distributions of nucleons in the deutron from $d(e, e'p)n$ reaction

[65] R. Machleidt, Phys. Rev. C**63**, 024001 (2001).

[66] R. Barlow and C. Beeston, Comp. Phys. Comm. **77**, 219 (1993).

[67] L. Lensniak, AIP Conf. Proc. 1030, 238–243 (2008). New formula for a resonant scattering near an inelastic threshold

[68] S. Agostinelli et al., Nuclear Instruments and Methods in Physics Research Section A: Accelerators, Spectrometers, Detectors and Associated Equipment **506**, 250 (2003).
J.Allison et el., Nuclear Instruments and Methods in Physics Research Section A: Accelerators, Spectrometers, Detectors and Associated Equipment **835**, 186 (2016).